BIOCHEMICAL PHARMACOLOGY 71 (2006) 426–440

available at www.sciencedirect.com

SCIENCE DIRECT®

journal homepage: www.elsevier.com/locate/biochempharm

Anticancer activity of the lanthanum compound [tris(1,10-phenanthroline)lanthanum(III)]trithiocyanate (KP772; FFC24)

Petra Heffeter[a], *Michael A. Jakupec*[b], *Wilfried Körner*[c], *Stefan Wild*[d], *Nikolai Graf von Keyserlingk*[e], *Leonilla Elbling*[a], *Haralabos Zorbas*[d], *Alla Korynevska*[f], *Siegfried Knasmüller*[a], *Hedwig Sutterlüty*[a], *Michael Micksche*[a], *Bernhard K. Keppler*[b], *Walter Berger*[a,*]

[a] *Institute of Cancer Research, Department of Medicine I, Medical University Vienna, Borschkegasse 8a, 1090 Vienna, Austria*
[b] *Institute of Inorganic Chemistry-Bioinorganic, Environmental and Radiochemistry, University of Vienna, Vienna, Austria*
[c] *Institute for Geological Sciences, University of Vienna, Vienna, Austria*
[d] *Institute of Biochemistry, Ludwig-Maximilian University of Munich, Munich, Germany*
[e] *Faustus Forschungs Compagnie GmbH, Leipzig, Germany*
[f] *Department of Regulation of Cell Proliferation, Institute of Cell Biology, National Academy of Sciences of Ukraine, Lviv, Ukraine*

ARTICLE INFO

Article history:
Received 12 October 2005
Accepted 9 November 2005

Keywords:
Lanthanum
1,10-Phenanthroline
Cell cycle arrest
Anticancer activity
Apoptosis

Abbreviations:
CDDP, cisplatin
ICP-MS, inductively coupled plasma mass spectroscopy
KP772, [tris(1,10-phenanthroline) lanthanum(III)]trithiocyanate
MTD, maximum tolerated dose
MTX, methotrexate

ABSTRACT

Aim of this study was to investigate the anticancer properties of the new lanthanum compound [tris(1,10-phenanthroline)lanthanum(III)]trithiocyanate (KP772; FFC24). In vitro, growth inhibition by KP772 was comparable for >60 tumour cell models with IC_{50} values generally in the low μM range. KP772 induced tumour cell apoptosis indicated by chromatin condensation, caspase substrate cleavage and mitochondrial membrane depolarisation. DNA is unlikely to represent the primary molecular target of KP772, as no significant interaction or damage of DNA was detectable both in vitro and in living cells. Moreover, we found no evidence for induction of radical species. In contrast, KP772 potently inhibited DNA synthesis paralleled by a massive block of cell cycle in G_0/G_1 phase and a selective decrease of cyclin B_1. Although treatment with KP772 induced expression of p53 and $p21^{Waf1}$, transfection of wild-type p53 into knock-out cells only marginally enhanced the cytostatic activity of KP772. In vivo, the anticancer activity of KP772 against human DLD-1 colon carcinoma xenografts was comparable to that of cisplatin and methotrexate at doses not causing significant adverse effects. With regard to toxicity, the LD_{50} and no-observed-adverse-effect levels (NOAEL) of KP772 in Sprague–Dawley rats were 21.6 and 7.5 mg/kg, in outbred albino mice 62 and 10 mg/kg, respectively. In summary, KP772 exerts anticancer activity via potent induction of cell cycle arrest and/or apoptosis and has promising in vivo anticancer activity against a human colon cancer xenograft. Together, these data suggest further development of KP772 as a new anticancer metal-drug.

* *Corresponding author*. Tel.: +43 1 4277 65173; fax: +43 1 4277 65169.
E-mail address: walter.berger@meduniwien.ac.at (W. Berger).
0006-2952/$ – see front matter © 2005 Elsevier Inc. All rights reserved.
doi:10.1016/j.bcp.2005.11.009

NCI, National Cancer Institute
1,10-phen, 1,10-phenanthroline
PI, propidium iodide
ROS, reactive oxygen species
TMAH, tetra methyl ammonium hydroxide

1. Introduction

Although platinum compounds have proved indispensable from the current systemic treatment of cancer only a few other transition metals including ruthenium and gallium have been more extensively investigated with regard to their potential quality as anticancer agents [1,2]. However, several observations suggest that also other metal-containing compounds might be suitable for the development of new chemotherapeutics. Such, simple lanthanum(III) salts have been reported to exert moderate anti-proliferative effects in vitro [3–6] and in vivo [7]. These effects are probably based on the inhibition of calcium fluxes, which are required for cell cycle regulation [4,7]. Moreover, lanthanide salts have recently been shown to cause mitochondrial breakdown, release of cytochrom *c* and induction of reactive oxygen species (ROS) [8]. Unfortunately, these activities are observed only at rather high concentrations.

The anticancer activity of lanthanum has, however, been distinctly enhanced by complexation with diverse ligands including chrysin [9], 1-aminocycloalkancarboxylic acid [10] and phenanthroline derivatives [11,12]. For most of these compounds, interactions with DNA involving intercalation or coordinative binding have been demonstrated [11,12]. However, the knowledge on the precise molecular mechanisms underlying their increased cytotoxic activity against cancer cells remains limited.

[Tris(1,10-phenanthroline)lanthanum(III)]trithiocyanate (KP772; FFC24) is a new compound, in which lanthanum centers a complex built by three 1,10-phenathroline molecules. The rational behind the synthesis of this compound is that besides lanthanum also the rigid planar 1,10-phenanthroline (1,10-phen) molecule has been demonstrated to exert distinct effects at least on in vitro cultured cells. Thus, 1,10-phen has been shown to stop DNA synthesis in CCRF-CEM and Ehrlich ascites cells leading to a cell cycle arrest in G_0/G_1 [13,14]. These effects were suggested to be based on the metal-chelating ability of 1,10-phen, especially affecting the availability of zinc, copper and iron [13,14]. Complexation with 1,10-phen has also been used to enhance the anticancer activity of several other metal ions including copper, ruthenium and cobalt (reviewed by [11,15,16]). Especially, several complexes of vanadium with 1,10-phen derivatives were reported to induce apoptosis and cell cycle arrest in vivo and in vitro [17–19]. In some cases, these effects were shown to be accompanied by induction of ROS [18].

In this paper, we demonstrate that KP772 is a promising new anticancer agent exerting potent activity against a wide range of tumour cell lines in vitro and a colon carcinoma xenograft model in vivo. Moreover, it is demonstrated that KP772 exerts anti-proliferative effects by distinct induction of cell cycle arrest in G_0/G_1 followed by induction of apoptosis, which is not mediated by DNA damage and radical formation.

2. Material and methods

2.1. Drugs

[Tris(1,10-phenanthroline)lanthanum(III)]trithiocyanate (KP772; FFC24; Fig. 1A) was prepared at the Institute of Inorganic Chemistry-Bioinorganic, Environmental and Radiochemistry, University of Vienna (Vienna, Austria) according to the procedure described by Hart and Laming [20]. For in vitro studies, the compound was dissolved in water and diluted into culture media at the concentrations indicated. For in vivo studies, KP772 was dissolved in physiological saline.

TMAH was purchased from Merck (Darmstadt, Germany). All other substances were purchased from Sigma–Aldrich (St. Louis, USA). All solutions were freshly prepared before use.

2.2. Cell culture

The following human cell lines were used in this study: the epidermal carcinoma-derived cell line KB-3-1, the promyelocytic leukaemia cell line HL60, the non-small cell lung cancer cell lines A549, VL-6 and VL-8, the small cell lung cancer cell line GLC-4, the glioblastoma U373, the hepatocellular carcinoma cell line Hep3B, and the breast cancer cell lines MCF7 and MDA-MB-231 (all donators are cited in ref. [21] and in ref. [22], A549, and Hep3B were derived from American Type Culture Collection, Manassas, VA). All cells were grown in RMPI 1640 supplemented with 10% fetal bovine serum. Cultures were regularly checked for *Mycoplasma* contamination.

2.3. Cytotoxicity assays and National Cancer Institute (NCI) cell line screen

Cells were plated (2×10^4 cells/ml for KB and Hep3B cells; 5×10^4 cells/ml for HL60 cells) in 100 μl per well in 96-well plates and allowed to recover for 24 h. Drugs were added in another 100 μl growth medium and cells exposed for 72 h. The proportion of viable cells was determined by an MTT-based vitality assay following the manufacturer's recommendations (EZ4U, Biomedica, Vienna, Austria). Cytotoxicity was expressed as IC_{50} values calculated from full dose–response curves (drug concentrations including a 50% reduction of cell survival in comparison to the control cultured in parallel

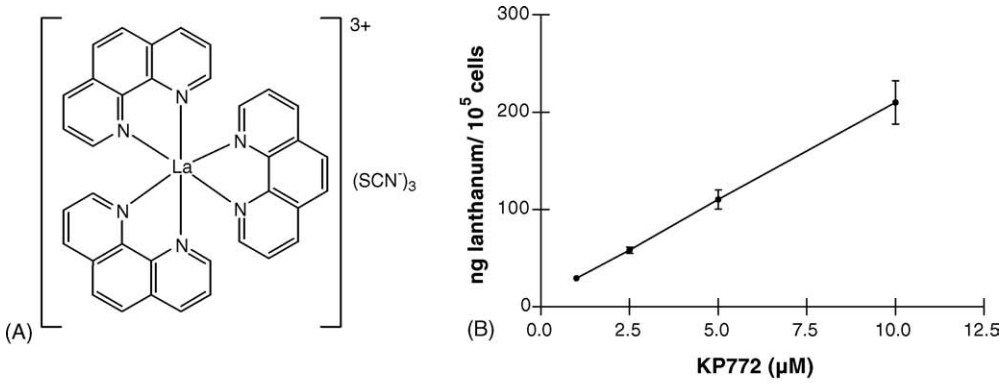

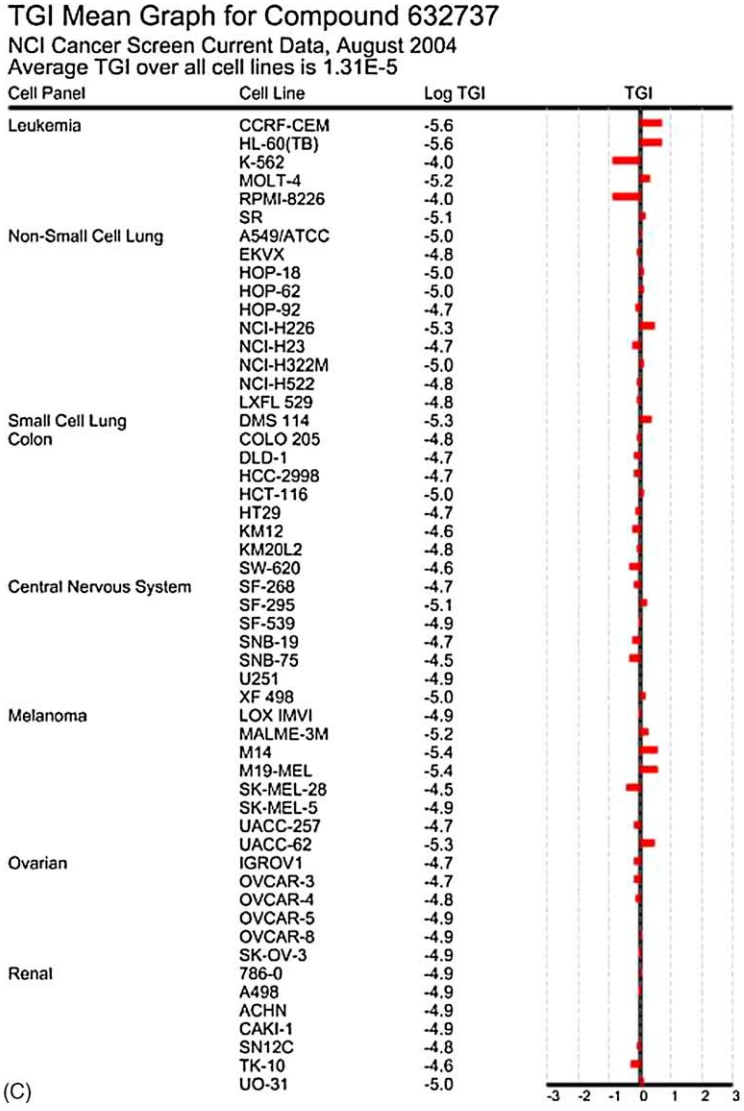

Fig. 1 – (A) [Tris(1,10-phenanthroline)lanthanum(III)]trithiocyanate (KP772; FFC24). (B) Intracellular accumulation of lanthanum in KB-3-1 cells after 1 h incubation with the indicated concentrations of KP772 measured by ICP-MS. (C) Anti-proliferative activity of KP772 (FFC24) in the National Cancer Institute anticancer screen. A graph of mean TGI profiles is shown. The bar scale is logarithmic. A bar extending to the right or to the left demonstrates enhanced or reduced sensitivity, respectively, of the cell line against KP772 as compared to the average sensitivity of all the cell lines tested. The converted actual concentration for the average $\log_{10}$ TGI value of 1.31E−5 is 12.2 μM.

without drugs). The methods used for the NCI 60 cell line anticancer drug screen have been described elsewhere [23]. Mean graphs were prepared from the appropriate data for each compound, and COMPARE correlation analyses were performed as described previously [24]. A detailed description is available at http://dtp.nci.nih.gov.

2.4. Toxicity of KP772

KP772 was administered by single intravenous application as a solution in 0.9% sodium chloride to outbred Swiss Albino mice and Sprague–Dawley rats. The studies were performed to determine the maximum tolerated dose (MTD), the medial lethal dose (LD_{50}) and the highest dose level, which caused no-observed-adverse-effects (NOAEL). Repeated dose analyses were done in Charles River athymic mice by application daily for 5 consecutive days. The MTD was evaluated on the basis of overt clinical symptoms reflecting adverse, drug-related side effects and body weight loss. Accepted toxicity was defined by the NCI as a mean group weight loss of less than 20% during the experiment and not more than 1 toxic death among 10 treated animals. The method was designated to meet the requirements of the Council Directive 2001/83/EC (28 November 2001), relating to medical products for human use, and of the Committee for Proprietary Medical Products CPMP/SWP/997/996 (23 July 1998). Details on the procedure can be obtained from the authors on request.

2.5. Evaluation of the antitumour effect of KP772 in vivo

Fragments of DLD-1 human colon adenocarcinoma (grown in donor mice) were transplanted subcutaneously into both flanks of the nude mice. Once tumours had reached a measurable size, mice were randomly allocated to either control or treatment groups, with six mice per group. Drugs were administered intravenously on days 0–4. Tumour sizes were measured regularly and the relative tumour volumes were calculated. Mann–Whitney *U*-tests were performed to determine the statistical significance of any differences in growth rate (based on tumour volume doubling time) between control and treated groups.

2.6. Drug accumulation assay

HL60 or KB-3-1 cells (1×10^5 per well) were exposed to 2.5 and 5 μM KP772 for 60 min at 37 and 4 °C. After three washes with PBS, cells were lysed by incubation in 400 μl TMAH at room temperature. Lysates were diluted in 0.6 N HNO_3 and lanthanum concentrations determined by inductively coupled plasma mass spectroscopy (ICP-MS) using an Elan 6100, Perkin-Elmer/Sciex Corporation. Values represent means of at least three independent experiments.

2.7. DNA intercalation assay

Intercalation of the tested drugs into salmon sperm DNA (Sigma) was determined using the methyl green assay as described [25]. Incubation times with test drugs were reduced to 2 h.

2.8. Investigation of changes of the global DNA secondary structure

Fifteen pmol of a pBluescript®II KS plasmid (2961 bp) were incubated in 480 μl TE buffer containing 60 μM of the tested drugs. For each time point (10 min to 72 h), 40 μl were removed and added to the same volume of 0.5 M NaCl and immediately frozen to −20 °C to inhibit further DNA binding. The plasmids were purified from unbound complexes and salt using a nick-column (Amersham Biosciences, Little Chalfont, UK). The sample volume was reduced in a speedvac and the solution adjusted to 5% glycerol, 0.5% SDS, 10 mM EDTA, 0.025% each of bromphenol blue and xylene cyanol. About 1 μg was loaded on a 1% agarose gel in tris/borate/EDTA buffer and separated by electrophoresis at 2 V/cm for 8 h. The gels were stained in tris/borate/EDTA buffer containing 0.2 mg/l ethidium bromide and photographed with an eagle-eye transilluminator (Amersham Biosciences).

2.9. Interstrand cross-link assay

0.9 pmol of a pBluescript®II KS plasmid (2961 bp) were linearised with *Hin*dIII, labelled with α-^{32}P-dATP by fill-in with Klenow polymerase and purified with a nick-column (Amersham Biosciences). 67.5 fmol of the fragment were incubated at 37 °C in 240 μl 0.1× TE buffer with 10 μM of KP772 or cisplatin. At each time point (1–72 h), 30 μl were removed and the reaction stopped by adjusting the NaCl concentration to 250 mM, followed by freezing at −20 °C. After purification with nick-columns (Amersham Biosciences), the samples were concentrated in a speedvac and adjusted to 2.5% Ficoll400, 50 mM NaCl, 2 mM EDTA, 0.025% bromcresol green. Cross-linked DNA was separated by electrophoresis in an alkaline 0.7% agarose gel (30 mM NaOH, 2 mM EDTA) at 2 V/cm over night. Prior to the autoradiography, the gel was fixed in a solution of 7% acetic acid and 4% glycerol and dried on a vacuum gel dryer.

2.10. Western blot analysis

Cell fractionation, protein separation and Western blotting were performed as described [26]. The following antibodies were used: anti-p53 monoclonal mouse DO-7 (NeoMarkers, CA, USA), dilution: 1:500; anti-$p21^{Waf1}$ polyclonal rabbit C-19 (Santa Cruz Biotechnology, CA, USA), dilution: 1:1000; Apoptosis Sampler kit: anti-PARP, anti-caspases 3 and 7, anti-cleaved caspases 7 (Cell Signalling Technology, Beverly, MA) rabbit polyclonal, dilution 1:1000; anti-cyclin A polyclonal rabbit sc-751 (Santa Cruz Biotechnology), dilution: 1:200; anti-cyclin B_1 monoclonal mouse sc-245 (Santa Cruz Biotechnology), dilution: 1:100; anti-cyclin D_1 monoclonal mouse sc-246 (Santa Cruz Biotechnology), dilution: 1:100; anti-β-actin monoclonal mouse AC-15 (Sigma), dilution: 1:1000. All secondary, peroxidase-labelled antibodies from Pierce were used at working dilutions of 1:10,000.

2.11. Cell cycle analysis

10^5 KB-3-1 or HL60 cells were seeded into 6-well plates, allowed to recover for 24 h, and then treated with 2.5 and 5 μM

KP772 or 1,10-phen. To analyse cell cycle distribution, cells were collected after 6, 12 and 24 h incubation and washed with PBS. Cells were fixed in 70% ethanol and stored at 4 °C. For analysis, cells were transferred into PBS, incubated with RNAse (10 μg/ml) for 30 min at 37 °C, treated with 5 μg/ml propidium iodide for 30 min and then analyzed by flow cytometry using FACS Calibur (Becton Dickinson, Palo Alto, CA). The resulting DNA histograms were quantified using the Cell Quest Pro software (Becton Dickinson and Company, New York, USA).

2.12. Mitochondrial membrane potential detection

Breakdown of the mitochondrial membrane potential ($\Delta\Psi_m$) was determined by FACS analysis using JC-1 (5,5,6,6-tetrachloro-1,1,3,3-tetraethylbenzimidazol-carbocyanine iodide), which allows to detect changes of the mitochondrial membrane potential ($\Delta\Psi_m$). For this purpose the Mitochondrial Membrane Potential Detection Kit (Stratagene, La Jolla, CA, USA) was used following the manufactures instructions. In short, 10^6 adherend KB-3-1 cells were treated overnight with the tested drugs. After trypsinisation and PBS washing, cells were incubated for 10 min in freshly prepared JC-1 solution (10 μg/ml in medium) at 37 °C. Spare dye was removed by washing in PBS and cell-associated fluorescence measured via FACS.

2.13. ^{3}H-thymidine incorporation assay

A549 cells (3×10^4 cells/ml) were seeded in a 96-well plate, and treated 24 h later with the drug for another 24 h. Medium was replaced by a 2 nM ^{3}H-thymidine solution (diluted in full culture medium; radioactivity: 25 ci/mM). After 4 h incubation at 37 °C, cells were washed three times with PBS. Cell lysates were prepared and the radioactivity determined as described [27].

2.14. Comet assay

The induction of DNA strand breaks was determined using the alkaline comet assay, according to the method described [28]. Each microscope slide was precoated with a layer of 1.5% normal melting point agarose and dried at room temperature. KB-3-1 cells were treated with drugs for 1 h, mixed with 100 μl of 0.5% low melting point agarose at 37 °C and dropped on top of the first layer. The agarose was allowed to solidify for 2 min on a cooled tray and then immersed in ice-cold lysing solution (2.5 M NaCl; 100 mM Na_2EDTA, 10 mM Tris–HCl, 1% Triton X-100; pH 10) for 1 h. After lysis, the slides were placed in a horizontal gel electrophoresis chamber and the DNA allowed to unwind for 1 h in the electrophoresis buffer (300 mM NaOH, 1 mM Na_2EDTA, pH 12.5). Electrophoresis was conducted for 20 min at 25 mV and 300 mA in a chamber cooled on ice. Then the slides were washed with neutralisation buffer (0.4 M Trizma Base, pH 7.5) and twice with water, fixed in 100% ice-cold methanol and stained with ethidium bromide. The comet tails were analysed using a fluorescent microscope (Nikon) with an automated image analysis system based on the public domain program NIH image analysis system [29]. DNA migration was expressed as comet tail length in micrometers according to guidelines [28]. Per experimental group, two slides were prepared and from each 50 cells were analysed. Cell viability at the time of assay was in all cases >90%.

2.15. P53 transfection

p53-positive cell clones were obtained from the p53(−/−) Hep3B cell line by transfection with the temperature-sensitive p53val143 vector [21]. To allow selection of transfected clones, cells were cotransfected with 1/10 amount of a pBabe puromycin resistance vector. For analysis of drug sensitivity, Hep3B/p53 and Hep3B/c (vector control) cells were plated on 96-well microstate plates at a density of 4×10^3/100 μl RPMI per well. After incubation for 24 h, cells were starved for another 24 h to reduce cell proliferation. On the next day, two test groups were defined: group 1 was transferred to 32 °C (wt p53) for 24 h, group 2 remained at 37 °C (mutated p53). Subsequently, drugs were added in 100 μl culture medium with 10% serum and after 1 h incubation the first group was transferred from 32 to 37 °C. Exposure was continued for another 72 h and cell viability was measured by EZ4U kit.

3. Results

3.1. Accumulation of KP772 in tumour cells

In order to examine whether KP772 is taken up by tumour cells, intracellular lanthanum levels were determined in KB-3-1 cells incubated in 1, 2.5, 5 and 10 μM KP772 for 1 h. About 2% of the total amount of drug could be localised in the cells. The intracellular amount of KP772 increased linearly in dose-dependent manner without any sign of plateau effect at the investigated doses (Fig. 1B). To clarify whether KP772 is actively or passively transported into cancer cells, the experiments were repeated at 4 °C. The reduction of temperature did not significantly attenuate drug uptake (Table 1) indicating lack of an active, ATP-dependent uptake mechanism for KP772.

3.2. Anticancer activity of KP772 in vitro

Anticancer activity of KP772 was examined using selected tumour cell lines from the stock of our laboratory (Table 2). Additionally, the anti-proliferative effects of KP772 were evaluated against a panel of 60 cell lines as part of the in vitro anticancer-screening services provided by the NCI. A detailed description of the protocol is available at http://dtp.nci.nih.gov.

Table 1 – Impact of temperature on intracellular accumulation of KP772 after 1 h treatment

Treatment (μM)	Lanthanum (ng) in 10^5 cells after 1 h			
	4 °C		37 °C	
	Mean[a]	±S.D.	Mean[a]	±S.D.
2.5	31.8	2.0	34.5	6.2
5	67.1	1.3	72.4	2.0

[a] Means of three independent experiments are given.

Table 2 – Cytotoxic activity of KP772 against various cell models at 72 h treatment

Cell line	Tissue	p53	IC_{75} (μM)		IC_{50} (μM)		IC_{25} (μM)	
			Mean[a]	±S.D.	Mean	±S.D.	Mean	±S.D.
A459	NSCLC[b]	wt	0.9	0.1	1.5	0.1	2.6	0.2
GLC-4	SCLC[c]	mut	1.5	1.4	2.0	1.6	3.0	1.7
Hep3B	Liver	(–/–)	1.3	0.5	2.2	0.8	>10.0	–
HL60	Leukaemia	(–/–)	0.9	0.8	1.2	0.9	1.5	1
KB-3-1	Cervix	mut	2.0	0.4	2.6	0.7	4.0	1.6
MDA-MB-231	Breast	mut	0.9	0.1	1.3	0.3	1.9	0.6
MCF7	Breast	wt	1.6	0.4	3.7	0.7	>10.0	–
U373	CNS[d]	mut	0.7	0.1	1.2	0.2	7.6	3.4
VL-6	NSCLC[b]	?	0.9	0.0	5.1	0.3	>10.0	–
VL-8	NSCLC[b]	?	0.9	0.1	1.5	0.1	2.6	0.2

[a] Means and S.D. of at least two independent experiments in triplicates.
[b] NSCLC, non-small cell lung cancer.
[c] SCLC, small cell lung cancer.
[d] CNS, central nervous system tumour.

In the NCI panel, KP772 had an overall mean GI_{50} (growth inhibition 50%) at 1.29 μM and a total growth inhibition (TGI) at 12.2 μM. The TGI concentrations of KP772 for the individual cell lines are presented in Fig. 1C. Generally, the IC_{50} and TGI values were remarkably similar independently of the cell models tested either at the NCI (Fig. 1C) or the Vienna lab (Table 2). When the NCI profile of KP772 was compared to that of other drugs, only moderate correlations (Pearson's correlation coefficients ≤ 0.427) to other known chemotherapeutics were observed. Notably, several anti-metabolic drugs including hydroxyurea and MTX were among those reaching significant correlations. This indicates that KP772 induced its anticancer activity in a manner which is new and widely different from other drugs.

3.3. *Anticancer activities of KP772 compared to lanthanum and 1,10-phen*

In Fig. 2A, dose–response curves for KP772 against KB-3-1 cells in comparison to the complex components 1,10-phen and $La(NO_3)_3$ at equimolar concentrations are shown. While 1,10-phen exerted modest anti-proliferative activity on its own, $La(NO_3)_3$ had no effect on the cancer cells at the concentrations used. KP772 was significantly more active than 1,10-phen with profound effects already below 2.5 μM.

3.4. *Characterisation of KP772-induced cell death*

In a first approach to characterise its anticancer activity, the impact of KP772 on nuclear morphology was assessed in KB-3-1 cells by DAPI staining. KP772 led to typical signs of apoptosis, i.e. condensed chromatin and fragmentation of nuclei into apoptotic bodies (Fig. 2B). Treatment with 5 μM KP772 for 24 h led to signs of apoptosis in 16% and 22% of KB-3-1 and HL60 cells, respectively. Correspondingly, a sub-G_0/G_1 peak in PI/FACS staining analysis appeared which is based on chromatin condensation in cells undergoing programmed cell death (compare Fig. 6B).

The fluorescent cationic dye JC-1 was used to detect the mitochondrial permeability transition as an early step in the induction of apoptosis by the intrinsic pathway [30]. In healthy, non-apoptotic cells the dye accumulates and aggregates within the mitochondria, resulting in bright red staining. In apoptotic cells, due to the collapse of the membrane potential, JC-1 cannot accumulate within the mitochondria and remains in the cytoplasm in its green-fluorescent monomeric form. In Fig. 2C, FACS analyses of JC-1-stained KB-3-1 cells treated with equimolar concentrations of KP772 and 1,10-phen are shown. Both compounds led to significantly increased proportions of apoptotic cells with 1,10-phen being slightly less efficient than KP772.

In order to further characterise KP772-induced cell death, the caspase-mediated cleavage of PARP (poly(ADP-ribosyl)polymerase), caspases 7 and 3 was analysed by Western blotting (Fig. 2D). After 24 h incubation with KP772, a dose-dependent increase of cleaved PARP and caspase 7 as well as loss of full-length caspase 3 was detectable. Taken together, these results indicate that KP772 exerts its cytotoxic activity by inducing apoptosis probably involving the mitochondrial pathway.

3.5. *KP772 and radical-induced DNA damage*

Many anticancer drugs like CDDP [31] and bleomycin [32] induce oxidative stress via generation of reactive oxygen species (ROS), which rapidly lead to DNA strand breaks. The alkaline comet assay was used to indicate whether ROS might be involved in the anticancer activity of KP772 (Fig. 3A). No change in the mean comet tail lengths was observed after 1 h treatment with KP772. In contrast, bleomycin used as a positive control at identical conditions increased DNA migration significantly ($p < 0.001$).

Additionally, we investigated the impact of the established radical scavenger *N*-acetyl cysteine (NAC) on the anticancer activity of KP772. Corroborating the data of the comet assay, NAC pre-treatment had no significant protective effect against the cytotoxic activity of KP772 in KB-3-1 cells while it potently attenuated bleomycin-induced cell death (Fig. 3B).

3.6. *Interaction of KP772 with DNA in vitro*

Intercalation into DNA is involved in the cytotoxic activity of several anticancer agents including anthracyclines [33]. In

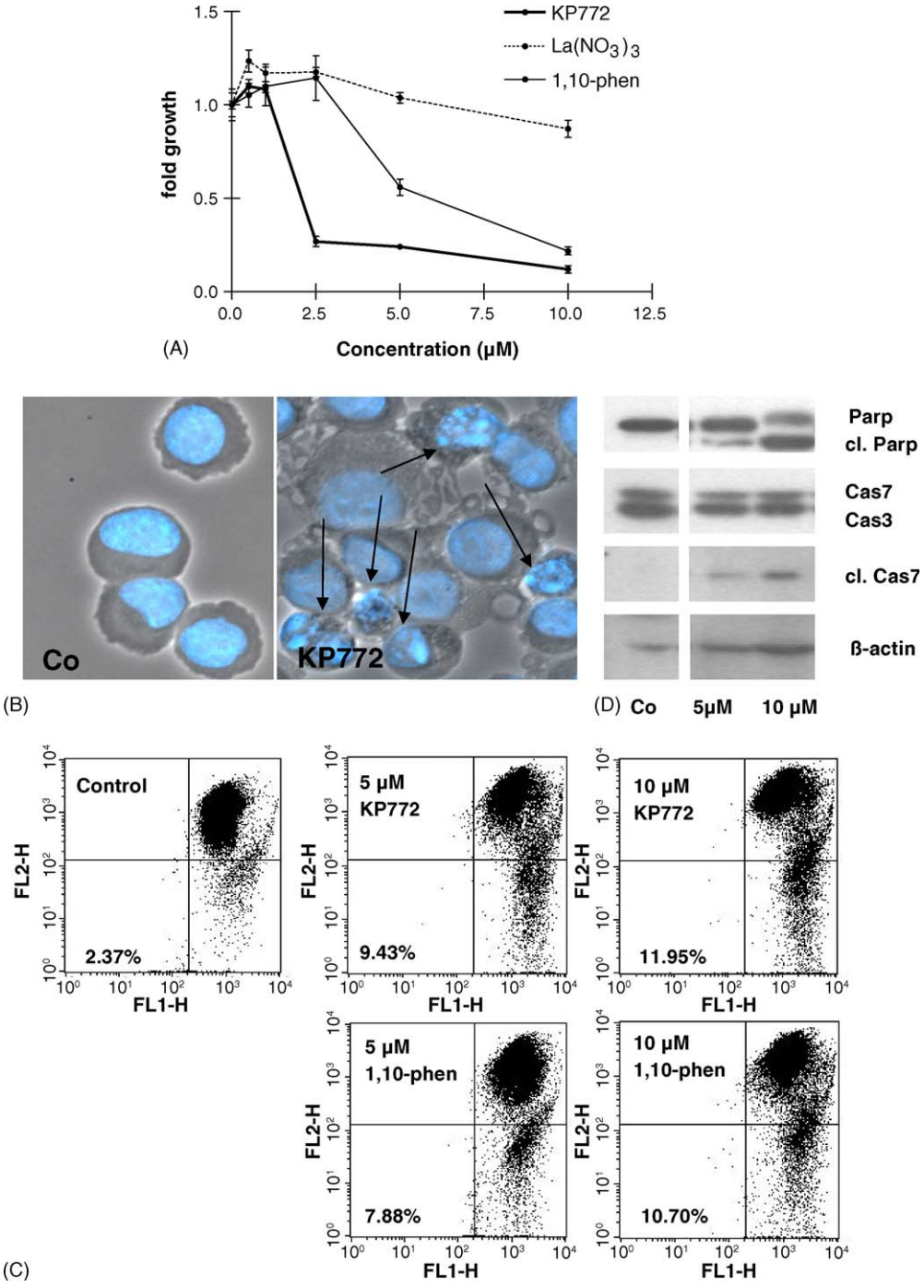

Fig. 2 – In vitro anticancer activity of KP772. (A) Dose–response curves of KB-3-1 cells after 72 h treatment with KP772, 1,10-phen or $La(NO_3)_3$ as indicated were measured by MTT assay. Values are given relatively to the untreated controls set as 1 and represent means and S.D. of two experiments in triplicates. (B) Induction of apoptosis in KB-3-1 cells after treatment with KP772 for 24 h. Staining of nuclei by DAPI in untreated controls or cells treated with 5 μM KP772. (C) Loss of mitochondrial membrane potential (JC-1 staining) after treatment with KP772 or 1,10-phen for 48 h. Percentages of apoptotic (green fluorescence, FL-1) cells, which are located in the right lower quarter, are given at the left bottom. (D) Caspase-induced cleavage of PARP, caspases 7 and 3 in KB-3-1 cells after 24 h treatment with KP772 as indicated was determined via Western blotting. Antibodies used are described in Section 2.

order to analyse whether also KP772 intercalates into double-stranded DNA, methyl green competition assays [25] were performed (Fig. 4A). Up to 300 μM KP772 (representing a 10-fold molar excess of the drug as compared to methyl green), only negligible indications for intercalation were observed while the positive control doxorubicin was highly active already at 15 μM. Interestingly, free 1,10-phen was more effective in competing with DNA bound methyl green than KP772.

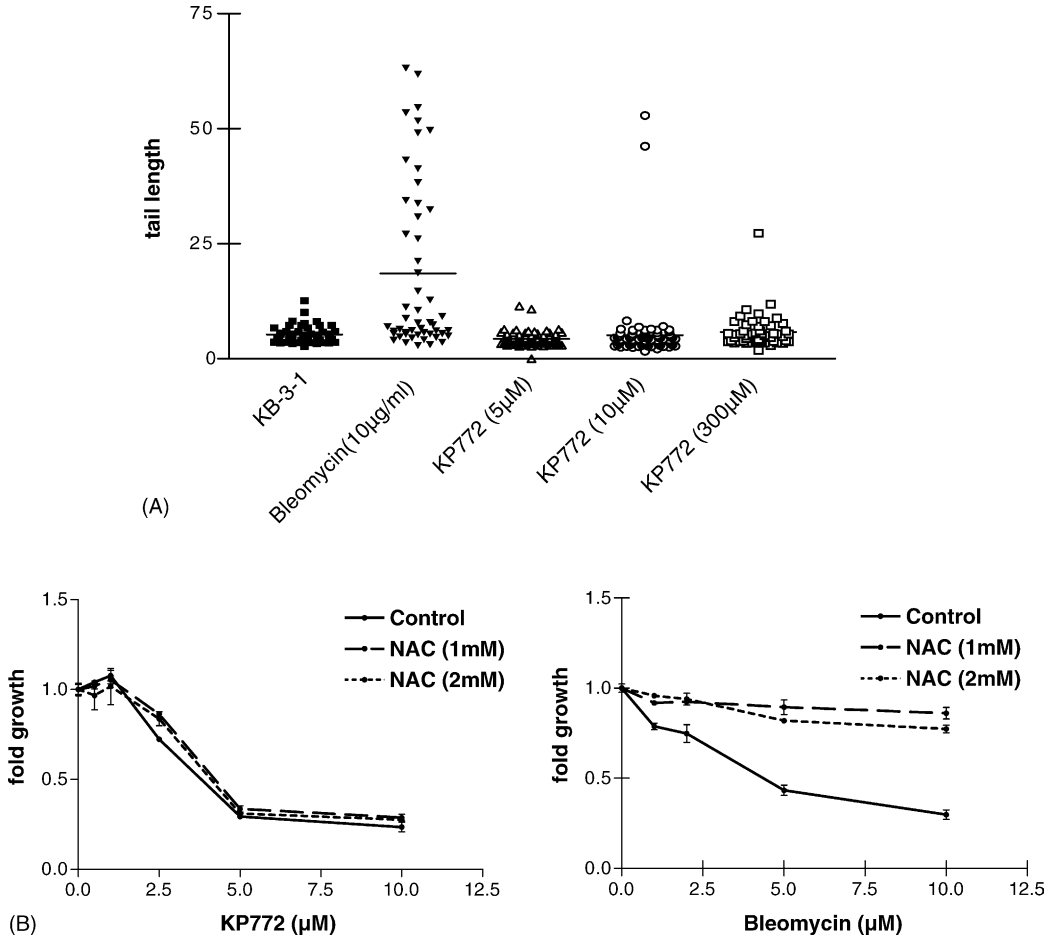

Fig. 3 – Treatment with KP772 does not induce DNA strand breaks and ROS formation. (A) Induction of DNA migration after 1 h treatment with the indicated concentrations of KP772 and bleomycin was analysed by the comet assay performed as described in Section 2. (B) Effects of 30 min pre-treatment with the radical scavenger NAC on the anticancer activity of KP772 or bleomycin (positive control) analysed by MTT assay.

Interstrand cross-links represent a key mechanism underlying the cytotoxic activity of CDDP [34,35] leading to inhibition of replication and/or transcription. Therefore, we analysed the in vitro DNA cross-linking ability of KP772 (Fig. 4B). In contrast to CDDP, only a very minor induction of cross-links was observed after treatment with KP772. Therefore, interstrand DNA cross-links are not likely to be responsible for the cytotoxic activity of KP772.

While bifunctional adducts of platinum drugs untwist and bend dsDNA [36,37] monofunctional ones [38] generally do not bend the DNA helix. Therefore, DNA untwisting and bending effects of KP772 were examined by monitoring the global changes of negatively supercoiled (SC) and ''open circular'' (OC) forms of plasmids, respectively [37]. Hence, a plasmid preparation containing both a covalently closed circular and an OC form was treated with 60 μM of each KP772 and CDDP (Fig. 4C). DNA untwisting by CDDP was revealed by relaxation of the SC. Reduced intensity of ethidium bromide staining with prolonged incubation might be the result of reduced intercalation through increased DNA platination [39]. In contrast to CDDP no untwisting activity of KP772 was obvious even at 72 h exposure time (Fig. 4C). Also non-periodic bending by CDDP was revealed by a faster migrating OC form, due to an apparent ''shortening'' of the contour length (Fig. 4C). In contrast, KP772 did not alter the DNA secondary structure. Instead, KP772 led to low but detectable cleavage of the DNA backbone after 48 h incubation. This was visible as increasing amount of the OC form of the plasmid during incubation with these compounds at the cost of the SC form (Fig. 4C).

3.7. *Impact of KP772 on cell cytoskeleton, DNA synthesis and cell cycle distribution*

When KB-3-1 cells were treated with KP772 their morphological appearance changed dramatically including a profound reorganisation of the microfilament system, and enhanced stress fibres with distinct focal adhesions (Fig. 5).

The effects of KP772 on DNA synthesis were determined by ^{3}H-thymidine incorporation assays. KP772 treatment dramatically inhibited ^{3}H-thymidine incorporation in A549 lung cells (Fig. 6A) already at 2.5 μM (24 h incubation), indicating a complete inhibition of DNA synthesis. To further characterise this stop in DNA synthesis, the effect of KP772 on cell cycle distribution of leukaemic HL60 cells was analysed (Fig. 6B). A significant reduction of cells in G_2/M

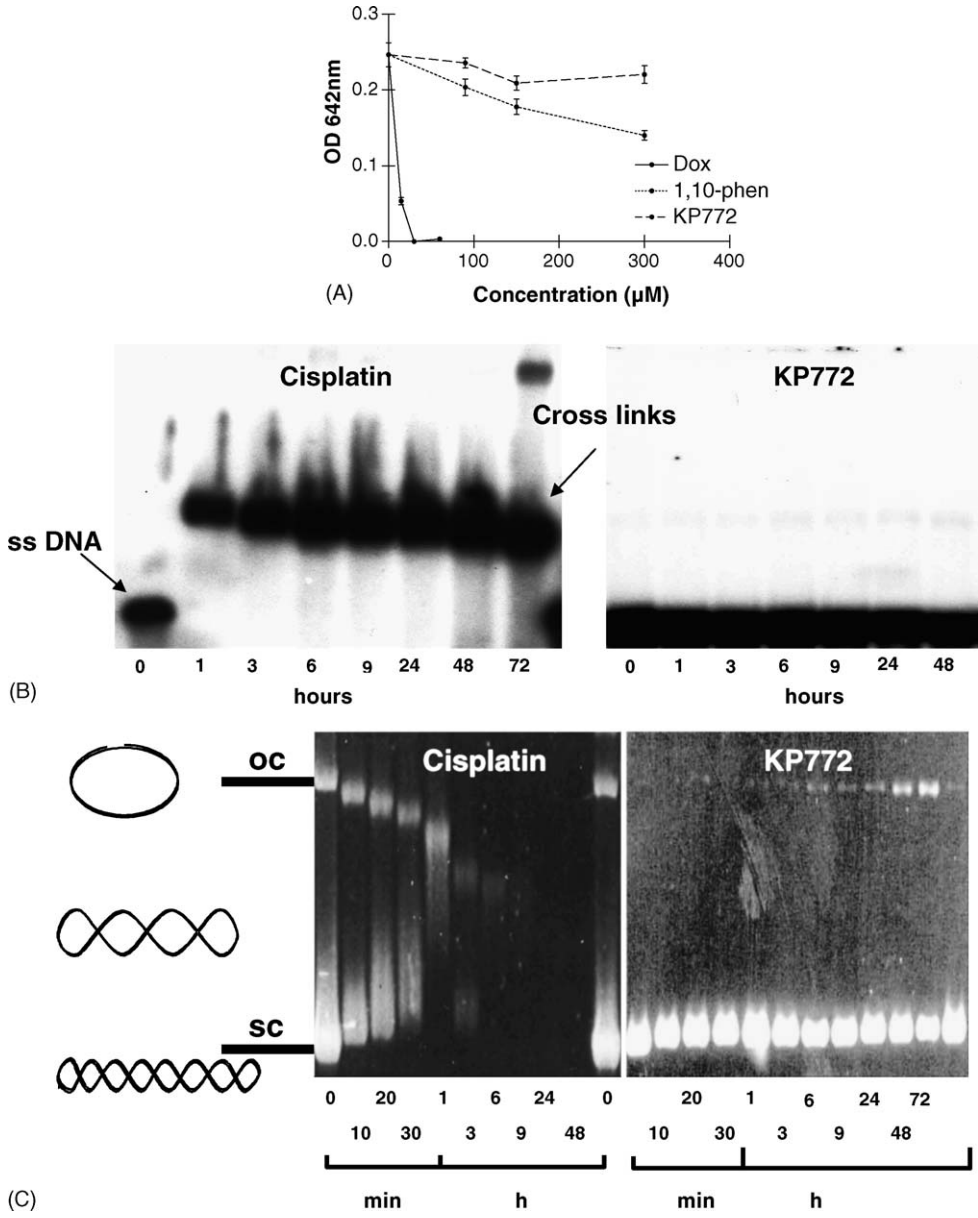

Fig. 4 – DNA intercalation, interstrand cross-links and changes of the DNA secondary structure by KP772. (A) After 1 h incubation with 30 μM methyl green, salmon sperm DNA (10 mg/ml) was treated for 2 h with the indicated drug concentrations. Absorbance was measured at 642 nm. Dose–response curves derived from two independent experiments in triplicates are shown. (B) Linearised, P^{32}-labelled plasmid DNA was treated with 10 μM CDDP or 10 μM KP772 for the indicated times (1–72 h), separated in agarose gels and analysed by autoradiography. DNA molecules with an interstrand cross-link are separated from single stranded DNA because of the higher molecular weight. (C) Plasmid DNA was treated with 60 μM each CDDP or KP772 for the indicated times, separated by agarose gel electrophoresis and stained with ethidiumbromide. Open circles (oc) and supercoiled plasmid (sc) DNA are indicated. With increasing reaction time, the open circles migrate faster due to non-periodic bending induced by platinum adducts. In contrast, the supercoiled DNA moves slower due to unwinding.

phase was already detectable following a 12 h treatment at 2.5 μM, while after 24 h almost no cells remained in S or G_2/M phase. In addition to the G_0/G_1 arrest, a significant proportion of cells had entered apoptosis indicated by the appearance of a sub-G_0/G_1 peak. Comparable results were observed in KB-3-1 cells (compare Fig. 7). The KP772-induced cell cycle arrest was accompanied by a profound, dose dependent reduction of cyclin B_1 and to a much lesser extent cyclin D_1 while cyclin A remained widely unchanged (Fig. 6C).

When compared to KP772, 1,10-phen was also able to induce a cell cycle arrest in the investigated cell types but less potently and after extended incubation times, only (Fig. 7; gated on living cells).

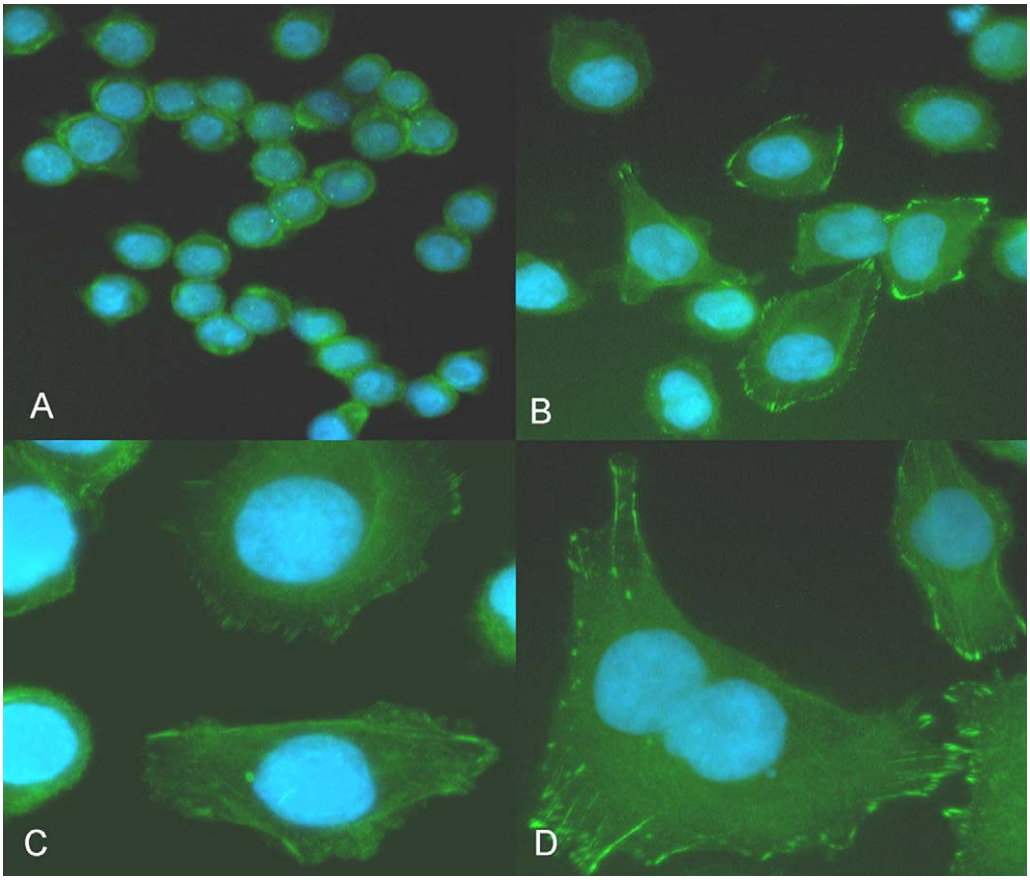

Fig. 5 – Impact of KP772 on the cell cytoskeleton. KB-3-1 cells were plated on chamber slides and either treated with the solvent (A) or KP772 at 2.5 μM (B and C) or 5 μM (D) for 24 h. Photomicrographs were taken using 40× (A and B) or 60× (C and D) oil objectives. DNA and microfilaments were visualised by DAPI and FITC phalloidin staining, respectively.

3.8. *Impact of the p53 status on KP772-induced cytotoxicity*

Wild-type P53 becomes activated in response to various types of stress and consequently arrests cell cycle predominantly in G_0/G_1 phase via induction of the cyclin-dependent kinase inhibitor $p21^{Waf1}$ [40]. Thus, we analysed whether treatment with KP772 induces p53 and $p21^{Waf1}$ in A549 cells containing wild-type p53 [41]. After 6 h treatment, dose-dependent p53 induction could be observed in the KP772-treated cells (Fig. 8A). $P21^{Waf1}$ upregulation became detectable only after 24 h treatment. Induction of $p53/p21^{Waf1}$ by bleomycin followed the same pattern but was distinctly stronger as compared to KP772.

Based on the upregulation of wild-type p53 by KP772 we used p53-null Hep3B-cells transfected with a temperature-sensitive p53 variant (Hep3B/p53) [21] to determine the contribution of wild-type p53 to the anticancer activity of KP772. In this cell, model the ectopic p53 is in mutant conformation at 37 °C and has wild-type conformation at 32 °C. Independent of the p53 status, Hep3B cell proliferation was significantly reduced at 32 °C leading to a distinctly decreased effect of KP772 (data not shown). To avoid the influence of temperature on cell growth, we reduced proliferation in all experimental groups by serum starvation 24 h prior to drug exposure. After a 1-h drug exposure, cells were returned to 37 °C to allow now unimpeded proliferation. Only at 1 μM KP772, a significantly enhanced cytotoxicity of KP772 against cells treated under wild-type p53 conditions was detectable (Fig. 8B). At higher drug concentrations, however, a weak opposite effect got obvious. This indicates that, although p53 expression is induced by treatment with KP772, it only weakly contributes to its anticancer activity.

3.9. *Toxicology of KP772*

The toxicity of KP772 after single intravenous application was investigated in outbred Swiss Albino mice and Sprague–Dawley rats and the maximal tolerated dose (MTD) based on approximate lowest lethal dose, the intravenous median lethal dose (LD_{50}) and the no observed adverse effects level (NOAEL) were calculated. In mice, the respective MTD, LD_{50} and NOAEL were 15, 62 and 10 mg/kg body weight. In case of rats, the respective parameters were 7.5, 21.6 and 7.5 mg/kg body weight. Common signs of systemic toxicity were hunched posture, pilo-erection and occasional body tremors. Repeated dose analyses were done in Charles River athymic mice by application daily for five consecutive days. KP772 was tolerated within NCI guidelines up to 10 mg/kg on this

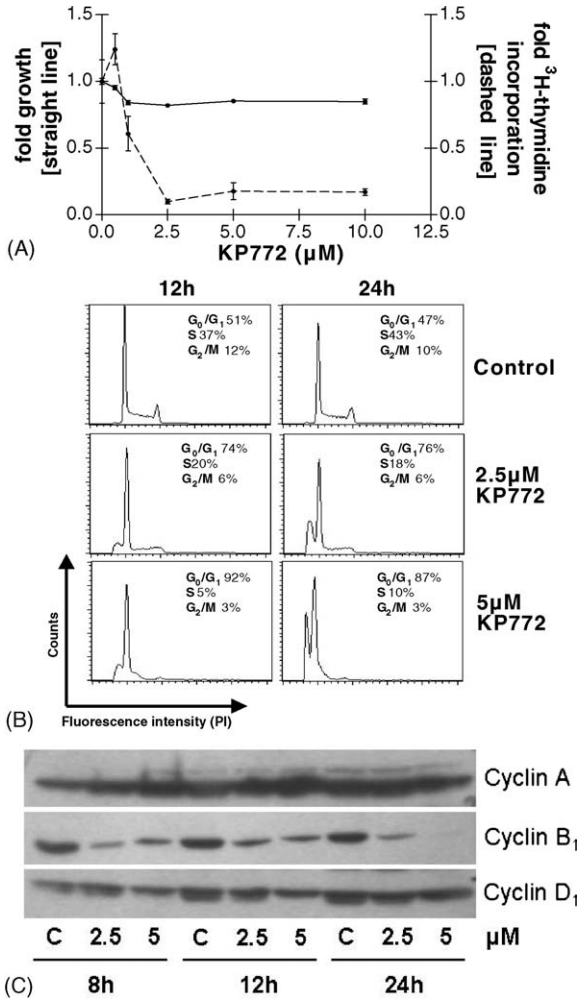

Fig. 6 – Impact of KP772 on DNA synthesis and cell cycle. (A) DNA synthesis and cell viability of A549 cells were determined by ^{3}H-thymidine incorporation and MTT assay, respectively, after 24 h treatment with KP772 at the indicated concentrations. (B) Changes in the cell cycle distribution of leukaemic HL60 cells treated with increasing concentrations of KP772 for the indicated times were analysed by PI staining and flow cytometry. Percentages of cells in G_0/G_1, S and G_2/M phase are indicated. (C) The impact of KP772 at the indicated concentrations on the expression pattern on cyclins in KB-3-1 cells was analysed by Western blot.

schedule. Detailed information on the evaluation procedures and the observed side effects can be obtained from the authors on request.

3.10. *In vivo anticancer activity of KP772 against a human colon carcinoma xenograft*

The in vivo anticancer activity of KP772, administered in a consecutive once-a-day (qd) × 5 schedule, is compared to MTX and CDDP in Fig. 9 and in Table 3. Growth of human DLD-1 colon cancer xenografts was significantly reduced by all three administered KP772 doses (4–12 mg/kg day) leading to a two-fold increased tumour doubling time. This effect was comparable to the ones of MTX and CDDP. While the effects of KP772 at 8 and 12 mg/kg did not differ significantly, 4 mg/kg were slightly less effective. As expected from the toxicology studies no severe side effects were observed at the used KP772 concentrations.

4. Discussion

The success of CDDP in the treatment of cancer patients led to the suggestion that also other metal complexes might be successfully included in future chemotherapy regimens. Although diverse new platinum compounds have been synthesised and in some cases developed to promising clinical application [17], attempts to use complexes with other metal centres have been comparably rare [42,43]. Here, we present preclinical data regarding to the use of the 1,10-phen-containing lanthanum compound, KP772 (FFC24), as an anticancer drug. In vitro, KP772 was demonstrated to be active against tumour cells of various origin including both solid and haematological malignancies. Additionally, the growth of the human colon adenocarcinoma xenograft DLD-1 was significantly reduced by KP772 with a potency comparable to those of MTX and CDDP. In cell biological assays, the anticancer activity of KP772 was demonstrated to be based on profound blockade of DNA synthesis, cell cycle arrest at the G_0/G_1–S phase border, and induction of apoptosis.

With respect to the in vitro anticancer activity of KP772, the relatively equal sensitivities of diverse tumour cell models including cell lines established from tumour specimen in our lab as well as the NCI panel were striking. The effective doses were almost generally in the low μM range and thus comparable to the ones already reported for other lanthanum complexes with 1,10-phen derivatives [11,12]. This suggests that KP772 targets in tumour cells a basic

Table 3 – Evaluation of the efficacy of KP772 in DLD-1 xenografts

Group	Mean time to RTV2 (days)[a]	Growth delay (days)	Significance (P)
Untreated control	3.1	–	–
KP772, 12 mg kg^{-1}, day × 5	6.5	3.4	<0.01
KP772, 8 mg kg^{-1}, day × 5	6.4	3.3	<0.01
KP772, 4 mg kg^{-1}, day × 5	5.5	2.4	<0.01
MTX, 4 mg kg^{-1}, day × 5	6.2	2.9	<0.01
CDDP, 2 mg kg^{-1}, day × 5	6.8	3.7	<0.01

[a] RTV2, relative tumour volume doubling time.

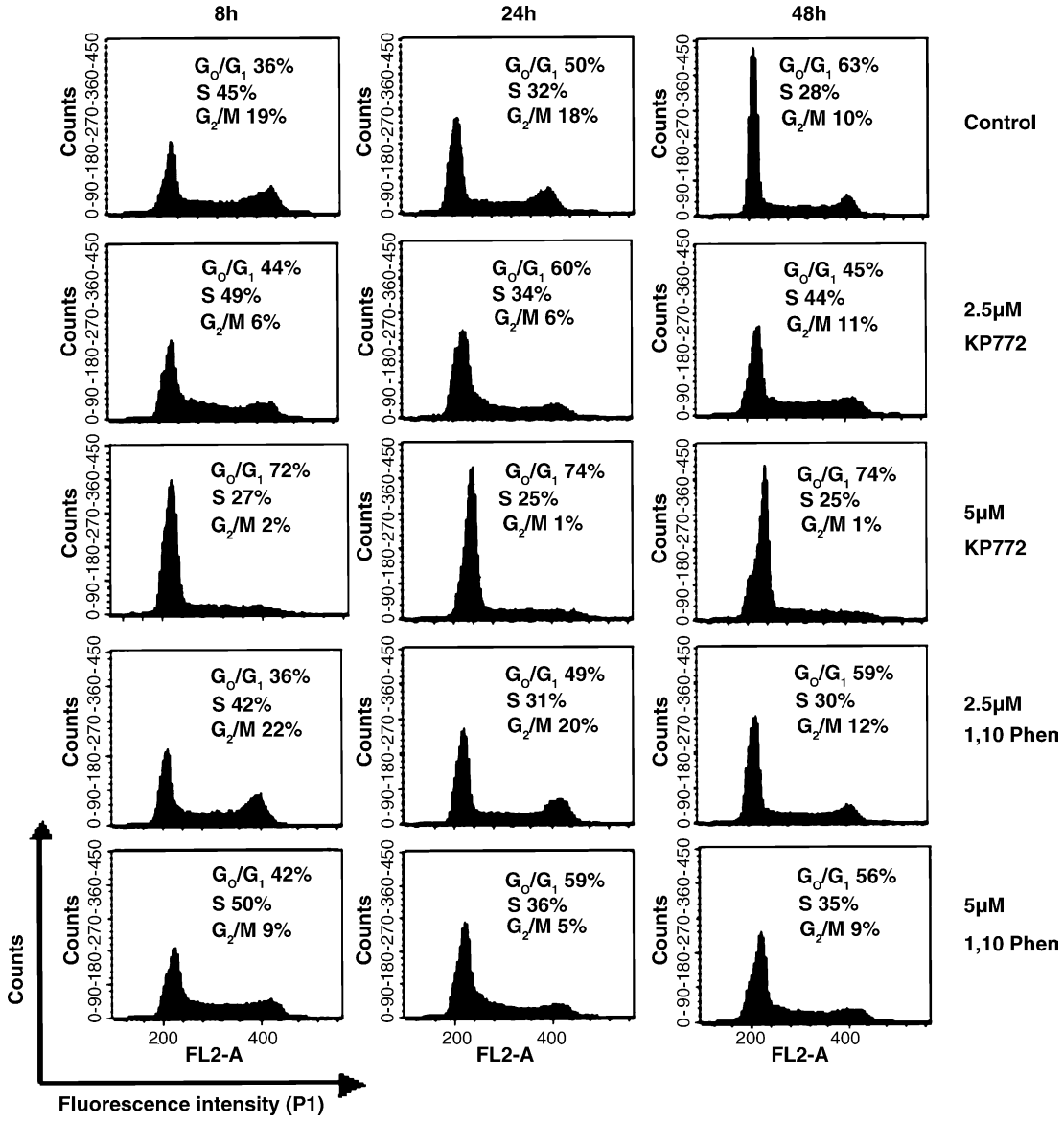

Fig. 7 – Effects of KP772 compared with 1,10-phen on cell cycle distribution of KB-3-1 cells were determine as described in Fig. 6B.

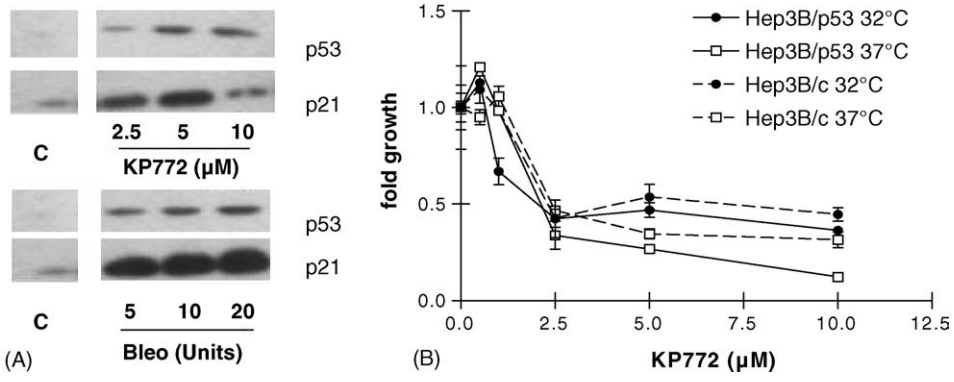

Fig. 8 – Impact of p53 of KP772 anticancer activity. (A) Induction of wild-type p53 and $p21^{Waf1}$ in A549 cells by treatment for 6 h and 24 h, respectively, with KP772 or bleomycin at the indicated concentrations was analysed via Western blotting. (B) Hep3B cells (p53−/−) were stably transfected with a vector containing a temperature-sensitive p53 gene (wild-type at 32 °C, mutated at 37 °C) (Hep3B/p53) or the control vector (Hep3B/c). Growth arrested cells were treated with KP772 as described in Section 2. Dose–response curves derived from two independent experiments in triplicates are shown.

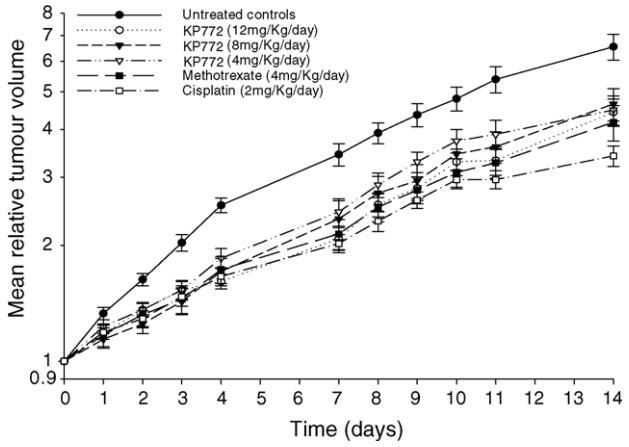

Fig. 9 – Activity of KP772 against a DLD-1 human colon adenocarcinoma xenograft in vivo. KP772 was administered and tumour size measured as described in Section 2. Values given are means and S.D. of six mice per experimental group.

mechanism, which is both equally present and equally vulnerable in all cell types investigated. Moreover, the comparable IC_{50} values for diverse cell models suggest that KP772 activity is not substantially affected by classical drug resistance mechanisms known to be present in several of the investigated cell lines [19]. Current investigations performed in our lab on the impact of resistance mechanisms confirmed the lack of interference of KP772 with ABC drug transporters (manuscript in preparation).

The molecular basis of the KP772 anticancer activity is currently unknown and matter of ongoing investigations. Based on the DNA cross-linking activity of platinum drugs [44] and the intercalating properties of 1,10-phen [15], we hypothesised that KP772 might primarily target the DNA. Unexpectedly, we found no clear-cut proof for any profound interaction of KP772 with DNA. In contrast to the positive control doxorubicin [33], significant DNA intercalation of KP772 was only detectable at very high drug concentrations (~100-fold IC_{50} in MTT assay). Moreover, KP772 exhibited a lower intercalating potency as compared to 1,10-phen despite the significantly higher anticancer activity of the lanthanum compound. This indicates the complexation of 1,10-phen with lanthanum reduced its DNA intercalating potency. Additionally, KP772 did neither sufficiently cross-link nor untwist plasmid DNA. Backbone stand breaks were only observed at a high concentration and after extended exposure time. These data argue against an important role of DNA interaction in the cytotoxic activity of KP772. Correspondingly, no indications for DNA damage by KP772 were obtained in living cells using the comet assays. This is in contrast to reports on DNA damaging activities of 1,10-phen copper and ruthenium complexes both demonstrated to potently cleave DNA [45,46]. Moreover, 1,10-phen vanadium derivatives were shown to induce ROS [47] resulting in DNA damage and apoptosis. A major contribution of oxidative stress to the cytotoxic activity of KP772 is unlikely as pre-treatment with the radical scavengers NAC did not protect cells against KP772 [48]. These data provide evidence that KP772 targets tumour cells via a molecular mechanism different from the ones of known metal 1,10-phen compounds.

Despite the lack of DNA damage we observed distinct cell cycle blockade in G_0/G_1 phase by KP772. During chemotherapy, accumulation of cells in G_0/G_1 is often the result of the respective cell cycle checkpoint activation as a consequence of DNA damage. Molecularly this process is often mediated by activation of p53 causing besides cell cycle arrest predominantly at G_1 phase also induction of apoptosis. Most of these p53 functions involve transcription factor activity resulting in enhanced expression of several anti-proliferative and pro-apoptotic proteins like for example the cyclin-dependent kinase inhibitor $p21^{Waf1}$ and the apoptosis inducing bax [40]. Despite the lack of DNA damage, we found induction of p53 and the downstream gene $p21^{Waf1}$ in p53-wild-type A549 cells. Correspondingly, several examples of DNA damage-independent induction of p53 for example as a consequence of nucleotide depletion, hypoxia and block of transcription have been reported [49]. However, in our hands p53-dependent signalling had only a minor influence on the cytotoxic activity of KP772, again suggesting that DNA damage is not the major cytostatic/toxic effect of KP772. Additionally, HL60 and Hep3B cells, which both are p53(−/−) [50], are highly sensitive to KP772-induced apoptosis. As also the p53(−/−) cells exhibited a distinct cell cycle arrest at G_1/S border, the upregulation of $p21^{Waf1}$ via p53 does not seem to be the predominant underlying mechanism. In agreement with this assumption, we found no induction of $p21^{Waf1}$ in KP772-treated p53(−/−) HL-60 cells (data not shown). Summarising, the profound cell cycle arrest of KP772-treated cells does not primarily depend on the activation of the respective cell cycle checkpoint via the $p53/p21^{Waf1}$ axis but on yet unknown mechanism. Most prominent were in our experiments the attenuated expression of cyclin B_1 and the profound reorganisation of the cell cytoskeleton. The elucidation of the precise interplay of the underlying molecular mechanisms is currently subject of ongoing experiments.

It is currently unknown whether the anticancer activity of KP772 is mainly determined by the lanthanum centre, by the 1,10-phen side chains or by specific properties of the complex. In contrast to CDDP, KP772 was demonstrated to be highly stable in aqueous solutions for several days (data not shown). Thus, it seems rather unlikely that high amounts of the very stable metal complex disaggregate in the cell environment within the relatively short time period until the cytotoxic effects become apparent. This does, however, not rule out that the complex might be metabolised in the cells making the presence of La^+ and/or 1,10-phen possible. This is of interest because for both parts of the complex anti-proliferative activities have been reported. Such, simple lanthanoid (mostly lanthanum) salts have been shown to inhibit cell cycle progression from G_0/G_1 to S phase in mitogen-stimulated normal mouse fibroblasts [3], murine melanoma cells [4] as well as in human leukaemia cells [5]. Moreover, lanthanum is a potent calcium antagonist, which might have an impact on the microfilament system [51]. This would suggest that KP772 exerts its activity mainly via the lanthanum centre. However, lanthanum salts are by far less effective as compared to KP772. Accordingly, in our experiments $La(NO_3)_3$ at 2.5–10 μM did not cause any substantial anti-proliferative activity while KP772

at equimolar concentrations induced potent cell cycle arrest and apoptosis. This suggests that the anticancer activity of KP772 is not only based on free lanthanum.

It also has to be kept in mind that, besides lanthanum, the rigid planar 1,10-phen moiety contained in the KP772 complex exerts relevant biological effects by itself. It was shown to intercalate in the DNA double helix and reversibly block cell cycle progression [13,14]. Additionally, it is a well-known chelator of intracellular metal ions (most prominently iron) and thus has been used as a potent inhibitor of ROS generation via the Fenton reaction [52]. At the first glance several of our observations suggest that the biological activities of KP772 might be partly based on those of free 1,10-phen. Thus, 1,10-phen, like KP772, blocked cell cycle in G_1/S phase, induced mitochondrial membrane depolarisation and consequently apoptosis. Moreover, chelation of iron led to potent upregulation of p53 [53]. However, several results strongly argue against that free 1,10-phen is solely responsible for the anticancer activity of KP772. First, KP772 exerts its effects on cell cycle more rapid and efficient as compared to 1,10-phen, which resembles in this respect other iron chelators including deferiprone or deferoxamine [54]. Second, despite its higher cytotoxic activity KP772 displayed lower DNA intercalating potency than 1,10-phen. Third, inhibition of ribonucleotide reductase as a consequence of iron chelation should lead to increased rather then decreased proportions of cells is S phase of the cell cycle as observed in case of KP772. Additionally, iron chelation was shown to induce necrosis and apoptosis [54] while we could not detect any LDH release following KP772 treatment (data not shown). Taken together these results suggest that KP772 synergistically integrates aspects of both lanthanum and 1,10-phen explaining its highly potent activity on tumour cells.

Summarising, our findings indicate that the novel lanthanum compound KP772 as a promising experimental anticancer drug. KP772 is readily taken up by tumour cells and exhibits potent and stable anti-proliferative and cytotoxic activities against diverse tumour types in vitro as well as against colon cancer xenograft in vivo. Our data suggest that the therapeutic potential of KP772 alone or in combination with other anticancer agents, should be assessed in further (pre)clinical studies.

Acknowledgements

We are indebted to Marlis Spannberger and Vera Bachinger for the skilful handling of cell culture, Elisabeth Rabensteiner, Rosa-Maria Weiss and Christian Balcarek for competent technical assistance, Paul Breit for preparing photomicrographs and Irene Herbacek for FACS analysis.

REFERENCES

[1] Galanski M, Arion VB, Jakupec MA, Keppler BK. Recent developments in the field of tumor-inhibiting metal complexes. Curr Pharm Des 2003;9:2078–89.
[2] Keppler BK, Pieper T. Studies into the mode of action of *trans*-HInd[$RuCl_4$(ind)$_2$] and *trans*-HIm[$RuCl_4$(im)$_2$]. In: Trautwein A, editor. Bioinorganic chemistry. Transition metals in biology and their coordination chemistry. Research report, DFG. Weihnheim/New York/Chichester: Wiley-VCH; 1997. p. 123–8.
[3] Estacion M, Mordan LJ. Competence induction by PDGF requires sustained calcium influx by a mechanism distinct from storage-dependent calcium influx. Cell Calcium 1993;14:439–54.
[4] Sato T, Hashizume M, Hotta Y, Okahata Y. Morphology and proliferation of B16 melanoma cells in the presence of lanthanoid and Al^{3+} ions. Biometals 1998;11:107–12.
[5] Dai Y, Li J, Li J, Yu I, Dai G, Hu A, et al. Effects of rare earth compounds on growth and apoptosis of leukemic cell lines. In Vitro Cell Dev Biol Anim 2002;38:373–5.
[6] Weiss H, Amberger A, Widschwendter M, Margreiter R, Ofner D, Dietl P. Inhibition of store-operated calcium entry contributes to the anti-proliferative effect of non-steroidal anti-inflammatory drugs in human colon cancer cells. Int J Cancer 2001;92:877–82.
[7] Anghileri LJ. Effects of gallium and lanthanum on experimental tumor growth. Eur J Cancer 1979;15:1459–62.
[8] Liu H, Yuan L, Yang X, Wang K. La(3+), Gd(3+) and Yb(3+) induced changes in mitochondrial structure, membrane permeability, cytochrome c release and intracellular ROS level. Chem Biol Interact 2003;146:27–37.
[9] Zeng YB, Yang N, Liu WS, Tang N. Synthesis, characterization and DNA-binding properties of La(III) complex of chrysin. J Inorg Biochem 2003;97:258–64.
[10] Kovachev TB, Ivanov DS, Buyukliev RT, Konstantinov SM, Karaivanova MC. Synthesis and tumor inhibiting activity of lanthanum(III) complexes with some 1-aminocycloalkancarboxylic acids. Pharmazie 1996;51:25–7.
[11] Wang ZM, Lin HK, Zhu SR, Liu TF, Zhou ZF, Chen YT. Synthesis, characterization and cytotoxicity of lanthanum(III) complexes with novel 1,10-phenanthroline-2,9-bis-alpha-amino acid conjugates. Anticancer Drug Des 2000;15:405–11.
[12] Wang ZM, Lin HK, Zhu SR, Liu TF, Chen YT. Spectroscopy, cytotoxicity and DNA-binding of the lanthanum(III) complex of an L-valine derivative of 1,10-phenanthroline. J Inorg Biochem 2002;89:97–106.
[13] Falchuk KH, Krishan A. 1,10-Phenanthroline inhibition of lymphoblast cell cycle. Cancer Res 1977;37:2050–6.
[14] Krishnamurti C, Saryan LA, Petering DH. Effects of ethylenediaminetetraacetic acid and 1,10-phenanthroline on cell proliferation and DNA synthesis of Ehrlich ascites cells. Cancer Res 1980;40:4092–9.
[15] Sammes PG, Yahioglu G. 1,10-Phenanthroline: a versatile ligand. Chem Soc Rev 1994;23:327–34.
[16] McFadyen WD, Wakelin LP, Roos IA, Leopold VA. Activity of platinum(II) intercalating agents against murine leukemia L1210. J Med Chem 1985;28:1113–6.
[17] Muggia FM, Fojo T. Platinums: extending their therapeutic spectrum. J Chemother 2004;16(Suppl. 4):77–82.
[18] Green DR. Apoptotic pathways: ten minutes to dead. Cell 2005;121:671–4.
[19] Szakacs G, Annereau JP, Lababidi S, Shankavaram U, Arciello A, Bussey KJ, et al. Predicting drug sensitivity and resistance: profiling ABC transporter genes in cancer cells. Cancer Cell 2004;6:129–37.
[20] Hart FA, Laming FP. Complexes of 1,10-phenanthroline with lanthanide chlorides and thiocyanates. J Inorg Nucl Chem 1964;26:579–85.
[21] Heffeter P, Pongratz M, Steiner E, Chiba P, Jakupec MA, Elbling L, et al. Intrinsic and acquired forms of resistance against the anticancer ruthenium compound KP1019. J Pharmacol Exp Ther 2005;312:281–9.
[22] Berger W, Elbling L, Hauptmann E, Micksche M. Expression of the multidrug resistance-associated protein (MRP) and

chemoresistance of human non-small-cell lung cancer cells. Int J Cancer 1997;73:84–93.
[23] Monks A, Scudiero D, Skehan P, Shoemaker R, Paull K, Vistica D, et al. Feasibility of a high-flux anticancer drug screen using a diverse panel of cultured human tumor cell lines. J Natl Cancer Inst 1991;83:757–66.
[24] Paull KD, Shoemaker RH, Hodes L, Monks A, Scudiero DA, Rubinstein L, et al. Display and analysis of patterns of differential activity of drugs against human tumor cell lines: development of mean graph and COMPARE algorithm. J Natl Cancer Inst 1989;81:1088–92.
[25] Schmeller T, Latz-Bruning B, Wink M. Biochemical activities of berberine, palmatine and sanguinarine mediating chemical defence against microorganisms and herbivores. Phytochemistry 1997;44:257–66.
[26] Berger W, Elbling L, Micksche M. Expression of the major vault protein LRP in human non-small-cell lung cancer cells: activation by short-term exposure to antineoplastic drugs. Int J Cancer 2000;88:293–300.
[27] Berger W, Elbling L, Minai-Pour M, Vetterlein M, Pirker R, Kokoschka EM, et al. Intrinsic MDR-1 gene and P-glycoprotein expression in human melanoma cell lines. Int J Cancer 1994;59:717–23.
[28] Tice RR, Agurell E, Anderson D, Burlinson B, Hartmann A, Kobayashi H, et al. Single cell gel/comet assay: guidelines for in vitro and in vivo genetic toxicology testing. Environ Mol Mutagen 2000;35:206–21.
[29] Helma C, Uhl M. A public domain image-analysis program for the single-cell gel-electrophoresis (comet) assay. Mutat Res 2000;466:9–15.
[30] Kim R, Emi M, Tanabe K. Role of mitochondria as the gardens of cell death. Cancer Chemother Pharmacol 2005;1–9.
[31] Naziroglu M, Karaoglu A, Aksoy AO. Selenium and high dose Vitamin E administration protects cisplatin-induced oxidative damage to renal, liver and lens tissues in rats. Toxicology 2004;195:221–30.
[32] Hoshino T, Nakamura H, Okamoto M, Kato S, Araya S, Nomiyama K, et al. Redox-active protein thioredoxin prevents proinflammatory cytokine- or bleomycin-induced lung injury. Am J Respir Crit Care Med 2003;168:1075–83.
[33] Baguley BC. DNA intercalating anti-tumour agents. Anticancer Drug Des 1991;6:1–35.
[34] Brabec V, Leng M. DNA interstrand cross-links of trans-diamminedichloroplatinum(II) are preferentially formed between guanine and complementary cytosine residues. Proc Natl Acad Sci USA 1993;90:5345–9.
[35] Roberts JJ, Friedlos F. Quantitative estimation of cisplatin-induced DNA interstrand cross-links and their repair in mammalian cells: relationship to toxicity. Pharmacol Ther 1987;34:215–46.
[36] Cohen GL, Bauer WR, Barton JK, Lippard SJ. Binding of *cis*- and *trans*-dichlorodiammineplatinum(II) to DNA: evidence for unwinding and shortening of the double helix. Science 1979;203:1014–6.
[37] Rice JA, Crothers DM, Pinto AL, Lippard SJ. The major adduct of the antitumor drug cis-diamminedichloroplatinum(II) with DNA bends the duplex by approximately equal to 40 degrees toward the major groove. Proc Natl Acad Sci USA 1988;85:4158–61.
[38] Brabec V, Reedijk J, Leng M. Sequence-dependent distortions induced in DNA by monofunctional platinum(II) binding. Biochemistry 1992;31:12397–402.
[39] Peritz A, Al-Baker S, Vollano JF, Schurig JE, Bradner WT, Dabrowiak JC. Antitumor and DNA-binding properties of a group of oligomeric complexes of Pt(II) and Pt(IV). J Med Chem 1990;33:2184–8.
[40] Oren M. Decision making by p53: life, death and cancer. Cell Death Differ 2003;10:431–42.
[41] Bai F, Matsui T, Ohtani-Fujita N, Matsukawa Y, Ding Y, Sakai T. Promoter activation and following induction of the p21/WAF1 gene by flavone is involved in G1 phase arrest in A549 lung adenocarcinoma cells. FEBS Lett 1998;437:61–4.
[42] Keppler BK, Henn M, Juhl UM, Berger MR, Niebl R, et al. New ruthenium complexes for the treatment of cancer. In: Progress in clinical biochemistry and medicine. Berlin, Heidelberg: Springer-Verlag; 1989. p. 41–69.
[43] Collery P, Keppler B, Madoulet C, Desoize B. Gallium in cancer treatment. Crit Rev Oncol Hematol 2002;42:283–96.
[44] Brabec V. DNA modifications by antitumor platinum and ruthenium compounds: their recognition and repair. Prog Nucleic Acid Res Mol Biol 2002;71:1–68.
[45] Pope LM, Reich KA, Graham DR, Sigman DS. Products of DNA cleavage by the 1,10-phenanthroline-copper complex. Inhibitors of *Escherichia coli* DNA polymerase I. J Biol Chem 1982;257:12121–8.
[46] Mei HY, Barton JK. Tris(tetramethylphenanthroline)ruthenium(II): a chiral probe that cleaves A-DNA conformations. Proc Natl Acad Sci USA 1988;85:1339–43.
[47] Dong Y, Narla RK, Sudbeck E, Uckun FM. Synthesis, X-ray structure, and anti-leukemic activity of oxovanadium(IV) complexes. J Inorg Biochem 2000;78:321–30.
[48] Zafarullah M, Li WQ, Sylvester J, Ahmad M. Molecular mechanisms of *N*-acetylcysteine actions. Cell Mol Life Sci 2003;60:6–20.
[49] Blagosklonny MV, Demidenko ZN, Fojo T. Inhibition of transcription results in accumulation of Wt p53 followed by delayed outburst of p53-inducible proteins: p53 as a sensor of transcriptional integrity. Cell Cycle 2002;1:67–74.
[50] Banerjee D, Lenz HJ, Schnieders B, Manno DJ, Ju JF, Spears CP, et al. Transfection of wild-type but not mutant p53 induces early monocytic differentiation in HL60 cells and increases their sensitivity to stress. Cell Growth Differ 1995;6:1405–13.
[51] Kunzelmann-Marche C, Freyssinet JM, Martinez MC. Regulation of phosphatidylserine transbilayer redistribution by store-operated Ca^{2+} entry: role of actin cytoskeleton. J Biol Chem 2001;276:5134–9.
[52] de Avellar IG, Magalhaes MM, Silva AB, Souza LL, Leitao AC, Hermes-Lima M. Reevaluating the role of 1,10-phenanthroline in oxidative reactions involving ferrous ions and DNA damage. Biochim Biophys Acta 2004;1675:46–53.
[53] Le NT, Richardson DR. The role of iron in cell cycle progression and the proliferation of neoplastic cells. Biochim Biophys Acta 2002;1603:31–46.
[54] Chenoufi N, Drenou B, Loreal O, Pigeon C, Brissot P, Lescoat G. Antiproliferative effect of deferiprone on the Hep G2 cell line. Biochem Pharmacol 1998;56:431–7.